Functionalization of Multiwalled Carbon Nanotubes with Poly(styrene-b-(ethylene-co-butylene)-b-styrene) by Click Coupling

ARTICLE *in* THE JOURNAL OF PHYSICAL CHEMISTRY C · JUNE 2010

Impact Factor: 4.77 · DOI: 10.1021/jp1028382

4 AUTHORS, INCLUDING:

Santosh K. Yadav
Drexel University
27 PUBLICATIONS **367** CITATIONS

SEE PROFILE

Sibdas Singha Mahapatra
Konkuk University
41 PUBLICATIONS **492** CITATIONS

SEE PROFILE

Functionalization of Multiwalled Carbon Nanotubes with Poly(styrene-*b*-(ethylene-*co*-butylene)-*b*-styrene) by Click Coupling

Santosh Kumar Yadav,[†] Sibdas Singha Mahapatra,[†] Jae Whan Cho,*[,†] and Jae Yeol Lee[‡]

Department of Textile Engineering, Konkuk University, Seoul 143-701, Korea, and Composite Group, Agency for Defense Development, Daejeon 305-600, Korea

Received: March 30, 2010; Revised Manuscript Received: May 25, 2010

Multiwalled carbon nanotubes (MWCNTs) were functionalized with poly(styrene-*b*-(ethylene-*co*-butylene)-*b*-styrene) triblock copolymer (SEBS) using click chemistry. Different compositions of SEBS-functionalized MWCNTs were obtained from reaction of azide moiety-containing SEBS on styrene units with alkyne-decorated MWCNTs. The SEBS-functionalized MWCNTs were characterized by FT-IR, Raman, XPS, SEM, and TEM measurements. The functionalized MWCNTs showed excellent dispersion in the SEBS matrix, and as a result, remarkably increased mechanical properties and high dielectric constants as well as enhanced thermal stability were obtained. The click coupled bonding of MWCNT with SEBS was very effective for controlling the material properties and achieving high performance materials.

1. Introduction

Poly(styrene-*b*-(ethylene-*co*-butylene)-*b*-styrene) (SEBS) may provide a broad platform for the development of multifunctional materials targeting a variety of applications such as actuators,[1] sensors,[2] biomaterials,[3] microcantact printing,[4] elastomers,[5] etc. SEBS functionalization with nanomaterials may lend more advantages in material properties due to the nanoscale structure and enhanced interaction of the reinforcing agent with the polymer matrix.[6] Higher dielectric constant[7,8] and enhanced mechanical properties[9,10] have been reported for applications such as actuators, capacitors, flexible electronics, and sensors by incorporating nanoparticles of TiO_2,[11,12] silver nanoparticles,[13] and ceramic[14] into the polymer matrix.

Carbon nanotubes (CNTs) have attracted enormous interest due to their excellent electrical, thermal, and mechanical properties.[15,16] Uniformly dispersed CNTs can be used as an ideal reinforcing agent for high strength polymer nanocomposites.[17] However, the challenging factor is dispersion of CNTs. This is strongly affected by strong van der Waals forces, which give rise to the formation of aggregates and inhibit the translation of nanophysical properties to nanocomposites. Many researchers have attempted to overcome these problems and have reported various methods for the preparation of polymer−CNT nanocomposites, such as melt mixing,[18] solution casting,[19] in situ polymerization,[20] cross-linking,[21] and electrospinning.[22] One of the most promising ways to improve the CNT dispersion and interfacial bonding between CNTs and the polymer matrix is chemical functionalization of CNTs, which can induce covalent attachment of a polymer chain to the CNTs. Particularly, the grafting of polymers onto CNT is very effective, because the grafted polymers on the surface can prevent the aggregation of CNTs.[23,24]

For obtaining functionalized SEBS, chemical modification of a polystyrene (PS) block in SEBS block copolymers has been employed, including sulfonation,[25] phosphonation,[26,27] benzoylation,[28] and naphthylation.[29] When CNTs are used for functionalization of SEBS, the high reactivity of the phenyl ring of the PS block can also be exploited. Various strategies for covalent attachment of a polymer chain to CNTs have been suggested. Covalent functionalization of CNTs is usually achieved through acid treatment, oxidation, esterification, amidation, radial coupling, anionic coupling, and click coupling.[30,31] Particularly, click chemistry, has received much attention from researchers in the fields of organic synthesis and materials chemistry, following a report by Sharpless et al.[32] The Cu(I)-catalyzed [3 + 2] Huisgen cycloaddition reaction is the most successful variant between azide and alkyne moieties, forming a high yielding 1,4-substituted 1,2,3-triazole with an enormously high tolerance of functional groups and solvents under highly moderate reaction conditions.[33]

In this study, we demonstrate a successful route for covalent attachment of an azide-functionalized styrene ring of SEBS to alkyne-functionalized multiwalled carbon nanotubes (MWCNTs) via click coupling with enhanced mechanical and dielectric properties.

2. Experimental Section

2.1. Materials and Reagents. SEBS block copolymer with 30 wt % polystyrene was provided by Kraton polymers. Its polydispersity index was 1.2, and the number average molecular weight of SEBS was 68 000, as measured using gel permeation chromatography. MWCNTs used in this study were purchased from Iljin Nano Tech, Seoul, Korea. Their diameter and average length were about 10−20 nm and 20 μm, respectively. 1,3,5-Trioxane (trioxane, Aldrich), chlorotrimethylsilane (TCI), tin(IV) chloride (Aldrich), propargyl bromide (Aldrich), *p*-nitrophenol (Aldrich), tetrabutylammonium bromide (Aldrich), 3-methylbutyl nitrite (Aldrich), copper iodide (Aldrich), and 1,8-diazabicyclo[5,4,0]undecene-7-ene (DBU, Aldrich) were used without further purification.

2.2. Chloromethylation of SEBS Block Copolymer. Typically, 5.0 g of SEBS and 5.4 g of trioxane (60 mmol) were dissolved in 250 mL of chloroform in a flask to yield a clear solution, and 22.8 mL of chlorotrimethysilane (180 mmol) and 3 mL of tin(IV) chloride (25.8 mmol) were then added to the mixture at 0 °C, and the solution was stirred under the same

* Corresponding author: E-mail: jwcho@konkuk.ac.kr. Tel: +82-2-450-3513. Fax: +82-2-457-8895.
[†] Konkuk University.
[‡] Agency for Defense Development.

10.1021/jp1028382
Published on Web 06/14/2010

SCHEME 1: Synthesis of SEBS-Functionalized MWCNTs via Click Coupling

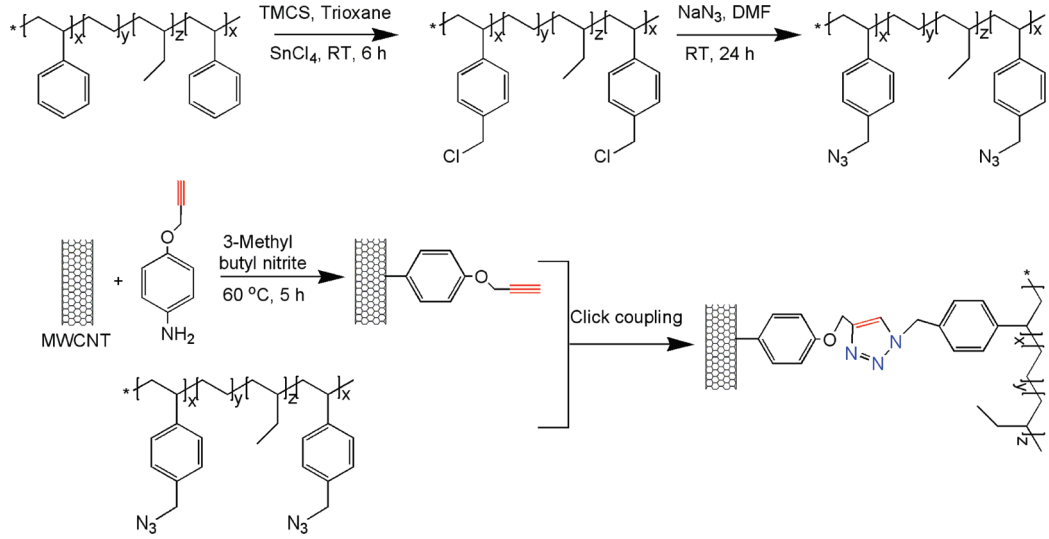

conditions for 30 min and further at room temperature for 6 h. After completion of the reaction, 100 mL of methanol/water solution (50% v/v) was added to stop the reaction. To obtain chloromethylated SEBS (SEBS-CH_2Cl), the reaction mixture was precipitated in methanol, purified by several iterations of dissolving/precipitation in chloroform/methanol, and dried overnight in a vacuum oven at room temperature.

2.3. Azidation of SEBS-CH_2Cl. In a typical reaction, 5.0 g of SEBS-CH_2Cl and 436 mg of NaN_3 (6.7 mmol) were added to 100 mL of dimethylformamide (DMF) in a flask, and the solution was stirred at room temperature for 24 h. The reaction mixture was precipitated in water to remove unreacted NaN_3 and dried overnight in a vacuum oven at room temperature.

2.4. Preparation of Alkyne-Functionalized MWCNTs. First, the *p*-aminophenyl propargyl ether was synthesized according to the literature procedure.[34] Alkyne-functionalized MWCNTs were synthesized initially; 160 mg of MWCNTs (13.33 mmol of carbon) and 7.85 g of *p*-aminophenyl propargyl ether (4 equiv/mol of carbon) were added in a two-necked flask with a reflux condenser and a magnetic stirrer bar under N_2 atmosphere conditions. Then, 7.81 g of 3-methylbutyl nitrite (5 equiv/mol of carbon) was slowly injected via a syringe, and the mixture was heated at 60 °C with continuous stirring for 5 h. The resulting product was washed with an excess amount of DMF and then diethyl ether to obtain alkyne-functionalized MWCNTs, and the final product was dried at 60 °C.

2.5. Synthesis of SEBS-MWCNTs by Click Coupling. Coupling of the azide moiety containing SEBS block copolymer (SEBS-CH_2N_3) and alkyne-functionalized MWCNTs was carried out via Cu(I)-catalyzed click chemistry. Ten milligrams of alkyne-functionalized MWCNTs was dispersed in 15 mL of DMF using bath sonication at room temperature for 10 min. The MWCNT solution was added to a two-necked flask containing 1 g of SEBS-CH_2N_3 solution in 15 mL of DMF with a reflux condenser and magnetic stirrer bar, and thereafter a homogeneous solution was obtained. After addition of 76.2 mg of copper iodide (0.40 mmol) and 3 g of 1,8-diazabicyclo[5,4,0]-undecene-7-ene (20 mmol), the solution was heated to 60 °C with continuous stirring for 24 h under a nitrogen atmosphere. After completing the reaction, the product was precipitated in methanol and further purified. The product was dried overnight under vacuum at room temperature, and the product yield was about 80−85% for all composition. Different compositions were obtained by varying the functionalized MWCNT amount, as represented in Table 2.

2.6. Measurements. Fourier transform infrared (FT-IR) spectroscopic measurements were performed using a JASCO FT-IR 300E device. ^1H NMR spectra were recorded in a Bruker 600 MHz NMR spectrometer using tetramethylsilane (TMS) as the internal standard and $CDCl_3$ as a solvent. Raman spectroscopy (LabRam HR Ar-ion laser 514 nm, Jobin-Yvon) was used to confirm the functionalization of MWCNTs. X-ray photoelectron spectroscopy (XPS, ESCSA 2000) was used to analyze the surface composition of the nanotubes. The surface morphology of pure and functionalized MWCNTs was observed by transmission electron microscopy (TEM, JEM 2100F, JEOL). The dispersion of MWCNTs in the composite was measured using a field emission scanning electron microscope (FE-SEM, S-4300SE, Hitachi). The mechanical properties of the nanocomposites were measured at an elongation rate of 10 mm/min at room temperature using a tensile tester machine (Instron 4468) with a dumbbell type specimen. The dimension of the test specimen was $60 \times 3 \times T$ mm^3, where T indicates the thickness. The dielectric constants and electrical conductivity of the samples were measured with a dielectric analyzer (Broadband Dielectric Analyzer, Novocontrol GmbH) in a frequency range of 10^{-1} to 10^7. Thermogravimetric analysis (TGA) was carried out in a TA Q 50 system TGA. The samples were scanned at a heating rate of 10 °C/min under flow of nitrogen.

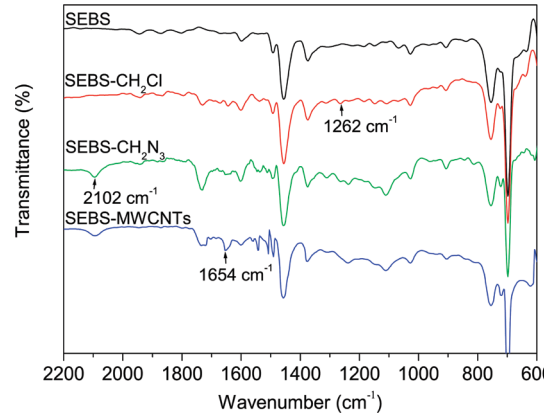

Figure 1. FT-IR spectra of SEBS, SEBS-CH_2Cl, SEBS-CH_2N_3, and SEBS-MWCNTs.

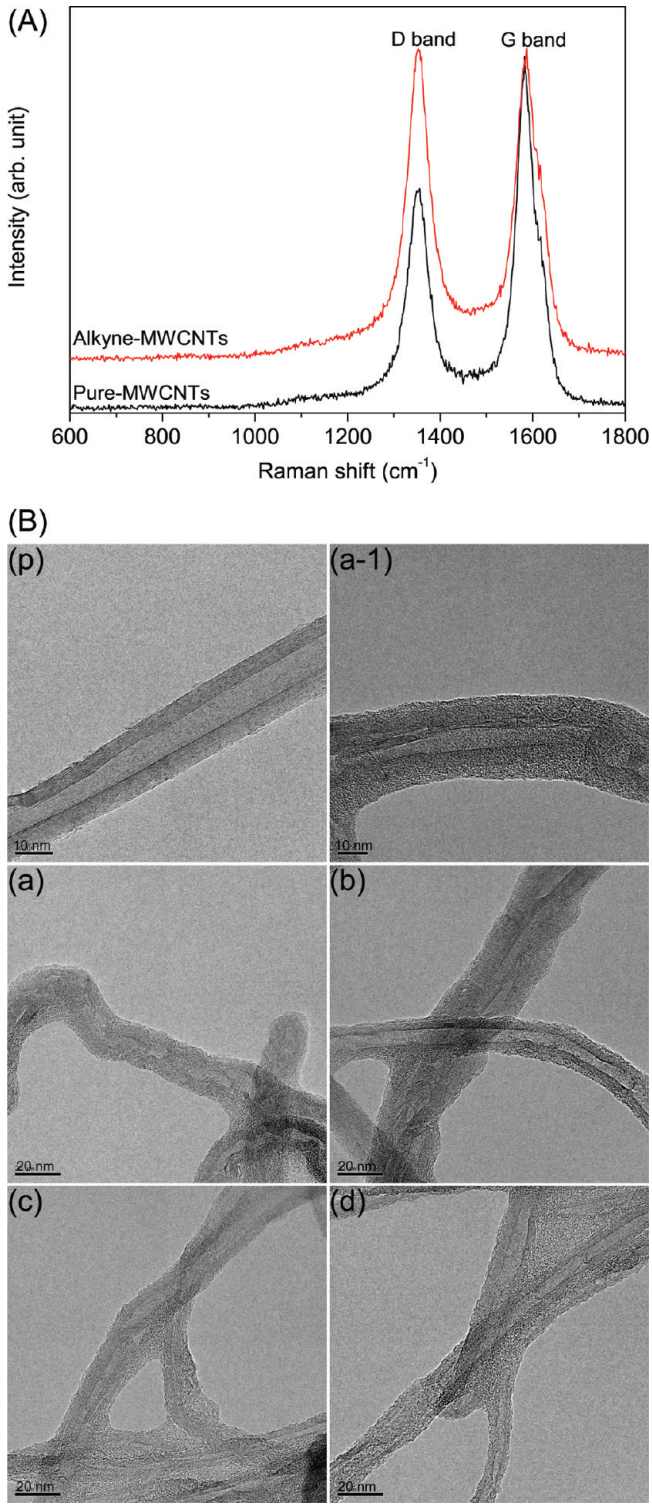

Figure 2. (A) Raman spectra of MWCNTs and (B) TEM images of pure MWCNTs (p), SEBS-MWCNT-1 (a and a-1), SEBS-MWCNT-2 (b), SEBS-MWCNT-3 (c), and SEBS-MWCNT-4 (d).

3. Results and Discussion

3.1. Functionalization of MWCNTs with SEBS. The covalently functionalized SEBS-MWCNTs in this study were prepared by click chemistry between azide-functionalized SEBS (SEBS-CH_2N_3) and alkyne-functionalized MWCNTs, as shown in Scheme 1. The alkyne-functionalized MWCNTs were prepared via the solvent free diazotization reaction and coupling reaction between MWCNTs and *p*-amino propargyl ether. The SEBS-CH_2Cl was prepared by Friedel−Craft reaction with stannic chloride as a catalyst in chloroform solution in the presence of trioxane and chlorotrimethylsilane.[35,36] Further azidation was accomplished by simple reaction of sodium azide in DMF (scheme 1). The extent of chloromethylation, i.e., 9.5 mol %, was determined from the ratio of the peak area of $-CH_2Cl$ to that of the benzene ring from the ^1H NMR spectra. The chemical modification of the SEBS, i.e., chloromethylation and azidation, was confirmed by ^1H NMR spectroscopy (Supporting Information, Figure S-1). The ^1H NMR spectrum of chloromethyleted SEBS (SEBS-CH_2Cl) showed the appearance of a new signal at 4.5 ppm corresponding to the $-CH_2Cl$ proton, confirming the chloromethylation of SEBS at the benzene ring. In the case of SEBS-CH_2N_3, it was observed that the signal at 4.5 ppm of SEBS-CH_2Cl shifted to 4.25 ppm, corresponding to $-CH_2$ linked with azide groups.[36]

The FT-IR spectra also showed the reaction results for SEBS-CH_2Cl, SEBS-CH_2N_3, and covalent functionalization of SEBS-MWCNTs, as shown in Figure 1. The IR peak around 1262 cm^{-1} due to C−Cl stretching for SEBS-CH_2Cl indicates chloromethylation of the SEBS.[36] The IR peak at 2102 cm^{-1} for SEBS-CH_2N_3 is due to the presence of the azide group, whereas the peak due to C−Cl stretching at 1262 cm^{-1} disappeared,[37] in the case of SEBS-MWCNTs the peak at 1654 cm^{-1} is due to the formation of triazole ring. These results are indicative of complete synthesis of SEBS-functionalized MWCNTs by click chemistry. However, the azide peak in SEBS-functionalized MWCNTs did not completely disappear due to excess amounts of azide group of SEBS.

Figure 2A shows Raman spectra of pure and alkyne-functionalized MWCNTs. Two characteristic bands are seen at 1585 cm^{-1} (G band) and 1352 cm^{-1} (D band).[38] The D band corresponds to defect sites in the hexagonal framework of MWCNTs due to disorder induced by sp^3 hybridization, whereas the G band indicates the presence of ordered sp^2 hybridization. The intensity ratio (I_D/I_G) values of pure MWCNTs and alkyne-functionalized MWCNTs were obtained as 0.62 and 0.98, respectively. The increase in the band intensity ratio (I_D/I_G) of the functionalized MWCNTs reflects the change of the hybridization of C atoms on the nanotubes from sp^2 to sp^3. The difference in the I_D/I_G values for pure and alkyne-functionalized MWCNTs is due to covalent functionalization of the alkyne group on MWCNTs. Figure 2B shows TEM images of MWCNTs and SEBS-functionalized MWCNTs. It can be seen that MWCNTs are wrapped by SEBS chains, providing strong evidence of well functionalized SEBS on the surface of the MWCNTs.

To elucidate the chemical structure and the organic proportion of SEBS-functionalized MWCNTs, XPS measurements were performed. Figure 3a shows XPS survey spectra of pure MWCNTs, SEBS, and SEBS-functionalized MWCNTs (SEBS-MWCNT-4). Two strong peaks at 285.0 eV (C 1S) and 531.6 eV (O 1S) are observed for both SEBS and SEBS-functionalized MWCNTs, and a new, relatively weak signal is also observed at 400.0 eV (N 1S) for SEBS-MWCNTs.[39] The relative atomic concentration of N for SEBS-functionalized MWCNTs was calculated as 3.2%, confirming the presence of a nitrogenous group in the sample (Table 1). The high resolution spectra N 1S of SEBS-functionalized MWCNTs displayed only one peak at 400 eV (Figure 3b), which suggests that only one kind of nitrogen atom is present due to the formation of a 1,2,3-triazole ring.[40,41] The slight excess azide residue in SEBS-MWCNTs, which has been discussed earlier, in the IR spectra might be degraded during the analysis.[41]

Furthermore, high resolution C 1S spectra of SEBS, pure MWCNTs, and SEBS-functionalized MWCNTs are presented

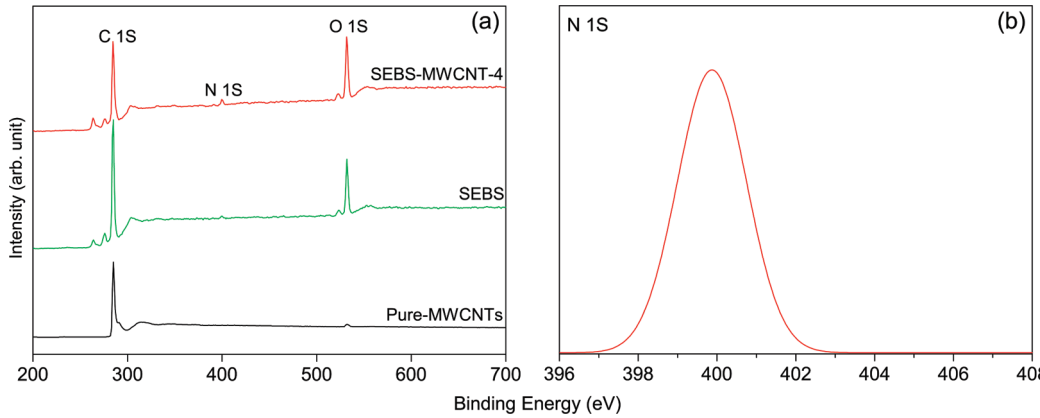

Figure 3. (a) XPS survey scan of pure MWCNTs, SEBS, and SEBS-MWCNT-4 and (b) high-resolution N 1S scan data of SEBS-MWCNT-4.

TABLE 1: Atomic Concentration of SEBS, Pure MWCNTs, and SEBS-MWCNTs Nanocomposites Determined from XPS Experimental Data

	atomic concentration (%)		
sample	C 1S	N 1S	O 1S
SEBS	85.1	0.6	14.3
pure MWCNTs	98.8	0.0	1.2
SEBS-MWCNT-4	76.1	3.2	20.7

in Figure S-2a−c, respectively (Supporting Information). The C 1S spectra of SEBS exhibited two characteristic peaks at 284.6

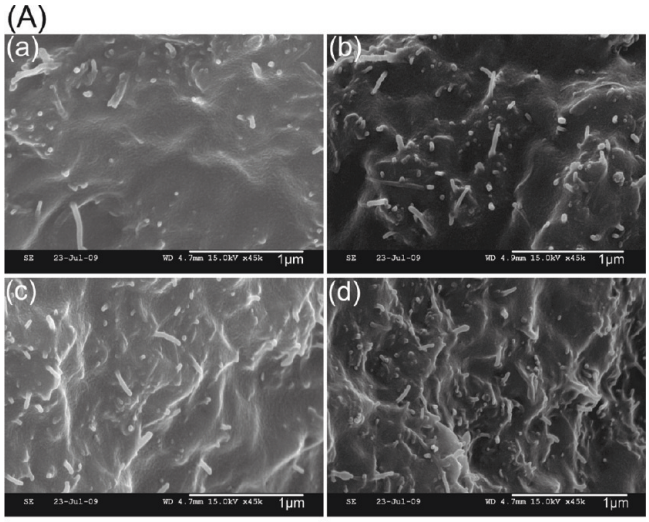

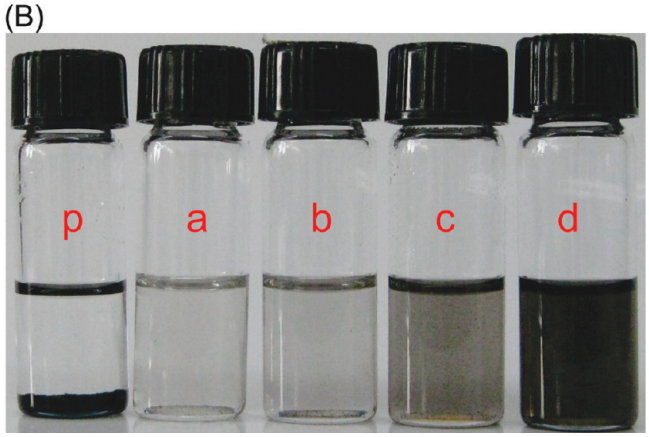

Figure 4. (A) FE-SEM images of SEBS-MWCNT-1 (a), SEBS-MWCNT-2 (b), SEBS-MWCNT-3 (c), and SEBS-MWCNT-4 (d) and (B) solubility test results of pure MWCNTs (p), SEBS-MWCNT-1 (a), SEBS-MWCNT-2 (b), SEBS-MWCNT-3 (c), and SEBS-MWCNT-4 (d).

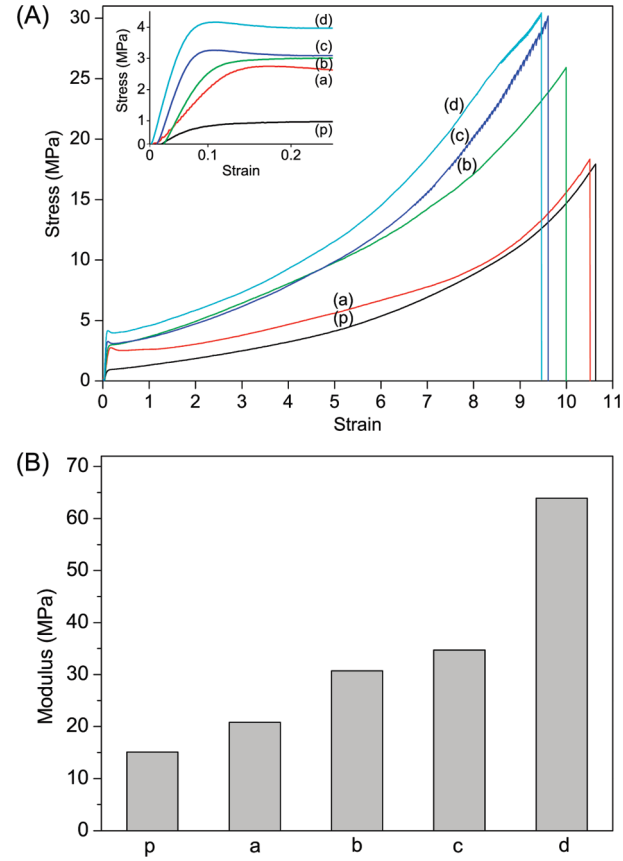

Figure 5. (A) Stress−strain curves and (B) modulus of SEBS (p), SEBS-MWCNT-1 (a), SEBS-MWCNT-2 (b), SEBS-MWCNT-3 (c), and SEBS-MWCNT-4 (d).

and 286.2 eV, corresponding to C—C and C—O—C, respectively. In contrast, the C 1S spectra of SEBS-functionalized MWCNTs exhibited three peaks corresponding to C—C (284.6), C—O—C (286.3), and C═O (288.0 eV), due to the presence of MWCNTs.[42] The relative atomic concentration of oxygen atoms of SEBS-functionalized MWCNTs is 20.7%, and the increased concentration of oxygen is due to the presence of the phenyl propargyl ether group on MWCNTs. This provides evidence of the covalent functionalization of MWCNTs with SEBS.

Figure 4A shows FE-SEM images of the cross section of the SEBS-functionalized MWCNTs. The MWCNTs are well dispersed, which is due to the covalent functionalization of MWCNTs with SEBS. The solubility of SEBS-functionalized MWCNTs was also observed in an organic solvent. Figure 4B shows the solubility test results of pure and SEBS-functionalized MWCNTs in toluene at a concentration of 2.5 mg/mL. It can

TABLE 2: Sample Formulation and Mechanical Properties of Composites

	feed weight (g)						
sample	SEBS-CH_2N_3	MWCNT-alkyne	breaking stress (MPa)	elongation-at-break	modulus (MPa)	yield stress (MPa)	yield strain
SEBS	1	0	17.8	10.6	15.1	0.9	0.12
SEBS-MWCNT-1	1	0.005	18.4	10.4	20.8	2.7	0.18
SEBS-MWCNT-2	1	0.01	25.8	9.9	30.7	2.9	0.15
SEBS-MWCNT-3	1	0.02	30.2	9.6	34.7	3.3	0.10
SEBS-MWCNT-4	1	0.03	30.4	9.4	63.9	4.1	0.10

be observed that the SEBS-functionalized MWCNTs show better dispersion stability than pure MWCNTs in toluene after 4 weeks. Thus, covalent functionalization can be a very effective means of dispersing carbon nanotubes in a polymer matrix.

3.2. Mechanical, Dielectric, and Thermal Properties of SEBS-Functionalized MWCNTs. Parts A and B of Figure 5 show the stress−strain curves and modulus of various SEBS-functionalized MWCNTs. All the MWCNT composites have a higher modulus and breaking strength than those of SEBS, which is due to the dramatic reinforcement effect of the covalent functionalized MWCNTs with SEBS matrix. This strengthening effect increased as the amount of MWCNTs was increased. Figure 5 and Table 2 present the improved modulus and breaking strength of the composites. For example, SEBS-MWCNT-4 showed approximately 4 and 1.7 times increased modulus and breaking stress, respectively. All the MWCNT composites also showed high elongation-at-break even though MWCNTs are incorporated, indicating the persistence of excellent stretchability of the composites, which is a key characteristic of elastomeric materials.

The dielectric constant of SEBS and SEBS-functionalized MWCNTs was measured as a function of frequency, as shown in Figure 6A. It increased with an increase of MWCNT content and decreased as the frequency was increased from 10^0 to 10^6 Hz. The SEBS-MWCNT-4 showed the highest dielectric constant of 6.1 at a frequency of 10^0 Hz, which is 3 times higher than that of SEBS. When the MWCNT concentration is low, that is, in the cases of SEBS-MWCNT-1 and SEBS-MWCNT-2, the dielectric constant was almost independent of frequency, because the electron polarization is effectively instantaneous. However, at higher MWCNT concentration for SEBS-MWCNT-3 and SEBS-MWCNT-4, the dielectric constant became frequency dependent. The dielectric constant also decreased as the frequency was increased from 10^0 to 10^6 Hz.[43] The ac conductivity of the composites are shown in Figure 6B. Their electrical conductivity increased with increasing MWCNT content.

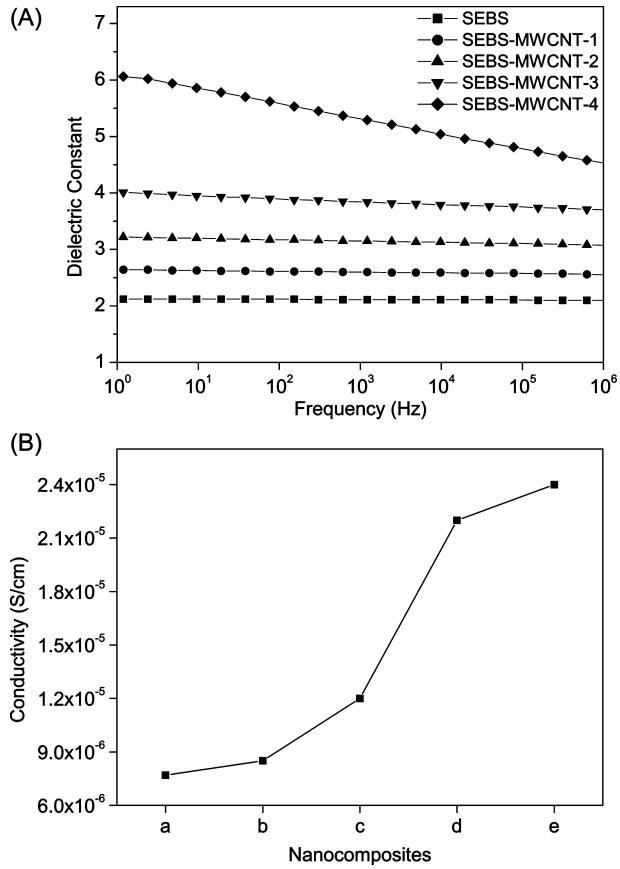

Figure 6. (A) Dielectric constants of the nanocomposites and (B) electrical conductivity of SEBS (p), SEBS-MWCNT-1 (a), SEBS-MWCNT-2 (b), SEBS-MWCNT-3 (c), and SEBS-MWCNT-4 (d).

The thermal degradation of composites was measured using a thermogravimetric analysis. The initial degradation temperature decreased proportionally with MWCNT content, as shown in Figure S-3 (Supporting Information). The carbon atoms of the MWCNTs attached to the SEBS are sp^3 hybridized, with high inherent strain, rendering them more susceptible to thermal degradation of the linkage between MWCNTs and SEBS in the initial stage of degradation.[44] However, at higher temperatures, the thermal stability of the composites increased, compared to that of SEBS. This is attributed to the barrier properties of the nanotubes, which are responsible for enhancing the thermal stabilization of the composites.

4. Conclusions

SEBS-functionalized MWCNTs have been synthesized successfully using click chemistry. The employment of covalent functionalization of SEBS with MWCNTs resulted in enhanced dispersion of MWCNTs in the polymer matrix. As a result, the SEBS-functionalized MWCNTs showed excellent mechanical properties and dielectric constant as well as enhanced thermal stability. Particularly, the breaking stress of the composites was highly increased while largely retaining the elongation-at-break, compared to that of SEBS. The present approach of click coupled MWCNTs with SEBS is a promising route for the development of high performance composites.

Acknowledgment. This work was supported by the Defense Acquisition Program Administration (DAPA) and the Agency for Defense Development (ADD). It is acknowledged that this research was also supported by the 2009 KU Brain Pool of Konkuk University.

Supporting Information Available: ^{1}H NMR spectra of the SEBS, SEBS-CH_2Cl, and SEBS-CH_2N_3 (Figure S-1), high-resolution C 1S scan data for SEBS, pure MWCNTs, and SEBS-MWCNTs (Figure S-2a, S-2b, and S-2c), and TGA thermograms of nanocomposites (Figure S-3). This material is available free of charge via the Internet at http://pubs.acs.org.

References and Notes

(1) Shankar, R.; Krishnan, A. K.; Ghosh, T. K.; Spontak, R. J. *Macromolecules* **2008**, *41*, 6100.

(2) Lipert, R. J.; Shinar, R.; Vaidya, B.; Pris, A. D.; Porter, M. D.; Liu, G.; Grabau, T. D.; Dilger, J. P. *Anal. Chem.* **2002**, *74*, 6383.
(3) Ranade, S. V.; Richard, R. E.; Helmus, M. N. *Acta Biomater.* **2005**, *1*, 137.
(4) Trimbach, D.; Feldman, K.; Spencer, N. D.; Broer, D. J.; Bastiaansen, C. W. M. *Langmuir* **2003**, *19*, 10957.
(5) Hadjichristidis, N.; Pispas, S.; Floudas, G. *Block Copolymers: Synthetic Strategies, Physical Properties, and Applications*, John Wiley and Sons: New York, 2002.
(6) Jung, Y. C.; Sahoo, N. G.; Cho, J. W. *Macromol. Rapid Commun.* **2006**, *27*, 126.
(7) Huang, C.; Zhang, Q.-M. *Adv. Mater.* **2005**, *17*, 1153.
(8) Carpi, F.; Gallone, G.; Galantini, F.; De Rossi, D. *Adv. Funct. Mater.* **2008**, *18*, 235.
(9) Yadav, S. K.; Mahapatra, S. S.; Cho, J. W.; Park, H. C.; Lee, J. Y. *Fibers Polym.* **2009**, *10*, 756.
(10) Sanui, K.; Kiyohara, Y.; Rikukawa, M.; Ogata, N. *React. Funct. Polym.* **1996**, *30*, 293.
(11) Carthy, D. N. M.; Risse, S.; Katekomol, P.; Kofod, G. *J. Phys. D: Appl. Phys.* **2009**, *42*, 145406.
(12) Yang, T.-I.; Kofinas, P. *Polymer* **2007**, *48*, 791.
(13) Huang, X.; Jiang, P.; Xie, L. *Appl. Phys. Lett.* **2009**, *95*, 242901.
(14) Gallone, G.; Carpi, F.; De Rossi, D.; Levita, G.; Marchetti, A. *Mater. Sci. Eng., C* **2007**, *27*, 110.
(15) Ajayan, P. M.; Stephan, O.; Colliex, C.; Trauth, D. *Science* **1994**, *265*, 1212.
(16) Moniruzzaman, M.; Winey, K. I. *Macromolecules* **2006**, *39*, 5194.
(17) Sahoo, N. G.; Jung, Y. C.; Yoo, H. J.; Cho, J. W. *Macromol. Chem. Phys.* **2006**, *207*, 1773.
(18) Tang, W.; Santare, M. H.; Advani, S. G. *Carbon* **2003**, *41*, 2779.
(19) Song, Y. S.; Youn, J. R. *Carbon* **2005**, *43*, 1378.
(20) Oliveira, M. M.; Zarbin, A. J. G. *J. Phys. Chem. C* **2008**, *112*, 18783.
(21) Jung, Y. C.; Yoo, H. J.; Kim, Y. A.; Cho, J. W.; Endo, M. *Carbon* **2010**, *48*, 1598.
(22) Sen, R.; Zhao, B.; Perea, D.; Itkis, M. E.; Hu, H.; Love, J.; Bekyarova, E.; Haddon, R. C. *Nano Lett.* **2004**, *4*, 459.
(23) Mahapatra, S. S.; Yadav, S. K.; Cho, J. W. *J. Nanosci. Nanotechnol* 2010 (in print).
(24) Yang, B.-X.; Shi, J.-H.; Pramoda, K. P.; Goh, S. H. *Compos. Sci. Technol.* **2008**, *68*, 2490.
(25) Barra, G. M. O.; Jacques, L. B.; Oréfice, R. L.; Carneiro, J. R. G. *Eur. Polym. J.* **2004**, *40*, 2017.
(26) Mayavan, S.; Choudhury, N. R.; Dutta, N. K. *Adv. Mater.* **2008**, *20*, 1819.
(27) Subianto, S.; Choudhury, N. R.; Dutta, N. K. *J. Polym. Sci., Part A: Polym. Chem.* **2008**, *46*, 5431.
(28) Wright, T.; Jones, A. S.; Harwood, H. J. *J. Appl. Polym. Sci.* **2002**, *86*, 1203.
(29) Jones, A. S.; Wright, T.; Smook, M. A.; Harwood, H. J. *J. Appl. Polym. Sci.* **2003**, *88*, 1289.
(30) Singh, P.; Campidelli, S.; Giordani, S.; Bonifazi, D.; Bianco, A.; Prato, M. *Chem. Soc. Rev.* **2009**, *38*, 2214.
(31) Zhang, Y.; He, H.; Gao, C.; Wu, J. *Langmuir* **2009**, *25*, 5814.
(32) Kolb, H. C.; Finn, M. G.; Sharpless, K. B. *Angew. Chem., Int. Ed.* **2001**, *40*, 2004.
(33) Wang, Q.; Chan, T. R.; Hilgraf, R.; Fokin, V. V.; Sharpless, K. B.; Finn, M. G. *J. Am. Chem. Soc.* **2003**, *125*, 3192.
(34) Li, H.; Cheng, F.; Duft, A. M.; Adronov, A. *J. Am. Chem. Soc.* **2005**, *127*, 14518.
(35) Li, T.; Ning, F.; Xie, J.; Chen, D.; Jiang, M. *Polym. J.* **2002**, *34*, 529.
(36) Ning, F.; Jiang, M.; Mu, M.; Duan, H.; Xie, J. *J. Polym. Sci., Part A: Polym. Chem.* **2002**, *40*, 1253.
(37) Wang, Y.; Chen, J.; Xiang, J.; Li, H.; Shen, Y.; Gao, X.; Liang, Y. *React. Funct. Polym.* **2009**, *69*, 393.
(38) Sato-Berrú, R. Y.; Basiuk, E. V.; Saniger, J. M. *J. Raman Spectrosc.* **2006**, *37*, 1302.
(39) Pei, X.; Hao, J.; Liu, W. *J. Phys. Chem. C* **2007**, *111*, 2947.
(40) Haensch, C.; Hoeppener, S.; Schubert, U. S. *Nanotechnology* **2008**, *19*, 035703.
(41) Al-Bataineh, S. A.; Britcher, L. G.; Griesser, H. J. *Surf. Sci.* **2006**, *600*, 952.
(42) Yu, H.; Jin, Y.; Peng, F.; Wang, H.; Yang, J. *J. Phys. Chem. C* **2008**, *112*, 6758.
(43) Saltas, V.; Vallianatos, F.; Soupios, P.; Makris, J. P.; Triantis, D. *J. Hazard. Mater.* **2007**, *142*, 520.
(44) Jana, R. N.; Cho, J. W. *J. Appl. Polym. Sci.* **2008**, *108*, 2857.

JP1028382